

Layer-by-Layer Transfer of Multiple, Large Area Sheets of Graphene Grown in Multilayer Stacks on a Single SiC Wafer

Sakulsuk Unarunotai,^{†,*,§,||} Justin C. Koepke,^{§,⊥} Cheng-Lin Tsai,^{*,§,¶} Frank Du,^{*,§,¶} Cesar E. Chialvo,^{*,#} Yuya Murata,^{*} Rick Haasch,^{*} Ivan Petrov,^{*,¶} Nadya Mason,^{*,#} Moonsub Shim,^{*,§,¶} Joseph Lyding,^{§,⊥} and John A. Rogers^{†,*,§,⊥,¶,∇,*}

[†]Department of Chemistry, [‡]Frederick Seitz Materials Research Laboratory, [§]Beckman Institute for Advanced Science and Technology, [⊥]Department of Electrical and Computer Engineering, [¶]Department of Materials Science and Engineering, [#]Department of Physics, [∇]Department of Mechanical Science and Engineering, University of Illinois at Urbana—Champaign, 1206 West Green Street, Urbana, Illinois 61801, and ^{||}Current address: Department of Chemistry, Faculty of Science, Chulalongkorn University, Bangkok 10330, Thailand.

Graphene¹ currently lies at the center of one of the most active fields of research in science and engineering, due to its exotic physics,^{2–4} to interesting challenges in its growth and, most importantly, to its promise for use in electronic systems of the future.^{5,6} The most widely explored form of graphene is obtained in small pieces, in a poorly controlled process of mechanical or chemical exfoliation from bulk pieces of graphite.^{1–4} Promising approaches to large area graphene include epitaxial growth on silicon carbide substrates (SiC),^{7–9} and chemical vapor deposition (CVD) on metal surfaces.^{10–12} Most envisioned applications require a scheme for transferring graphene from these growth substrates to substrates of interest for device integration. In the case of CVD, etching the metal releases the graphene and prepares it for transfer, using stamps or related processes.^{11–13} In this case, most demonstrations focus on use as transparent conducting films.^{11,13,14} By contrast, research in SiC centers on the formation of high performance transistors and circuits.^{15,16} This record of work, particularly when combined with schemes that might allow formation of ribbons of graphene by controlled growth on crystalline step edges,¹⁷ makes the SiC system interesting for further exploration in active electronic devices. Two recent reports describe methods for transfer of graphene from SiC;^{18,19} both rely on mechanical peeling rather than etching. In the first, thin films of Au deposited onto graphene grown on the Si-face of a SiC wafer provide the adhesion necessary for transfer.¹⁸ A thin, polymeric backing layer serves as a mechanically strong sup-

ABSTRACT Here we report a technique for transferring graphene layers, one by one, from a multilayer deposit formed by epitaxial growth on the Si-terminated face of a 6H-SiC substrate. The procedure uses a bilayer film of palladium/polyimide deposited onto the graphene coated SiC, which is then mechanically peeled away and placed on a target substrate. Orthogonal etching of the palladium and polyimide leaves isolated sheets of graphene with sizes of square centimeters. Repeating these steps transfers additional sheets from the same SiC substrate. Raman spectroscopy, scanning tunneling spectroscopy, low-energy electron diffraction and X-ray photoelectron spectroscopy, together with scanning tunneling, atomic force, optical, and scanning electron microscopy reveal key properties of the materials. The sheet resistances determined from measurements of four point probe devices were found to be ~ 2 k Ω /square, close to expectation. Graphene crossbar structures fabricated in stacked configurations demonstrate the versatility of the procedures.

KEYWORDS: graphene · silicon carbide · epitaxial growth · transfer technique · layer-by-layer · four-point measurement

port for the peeling process, in an overall scheme conceptually similar to those designed for the transfer of random networks and aligned arrays of single-walled carbon nanotubes.²⁰ Removal of the polymer and the Au using orthogonal etching methods after peeling and transferring to another substrate completes the process. This procedure separates the adhesive layer (*i.e.*, Au) from the structural component (*i.e.*, polymer), thereby allowing separate optimization of each. Examination of data from Raman spectroscopy, atomic force microscopy (AFM), X-ray photoelectron spectroscopy (XPS), and other techniques suggests the possibility for selective transfer of only the uppermost graphene layer on the SiC.¹⁸ Total areas are limited, however, by the moderate adhesion of Au to graphene. In another report, thermal adhesive tape was shown to enable large area transfers, but in a mode that removes almost all of the graphene layers (typically several) from the SiC.¹⁹

*Address correspondence to jrogers@illinois.edu.

Received for review August 4, 2010 and accepted September 08, 2010.

Published online September 15, 2010.
10.1021/nn101896a

© 2010 American Chemical Society

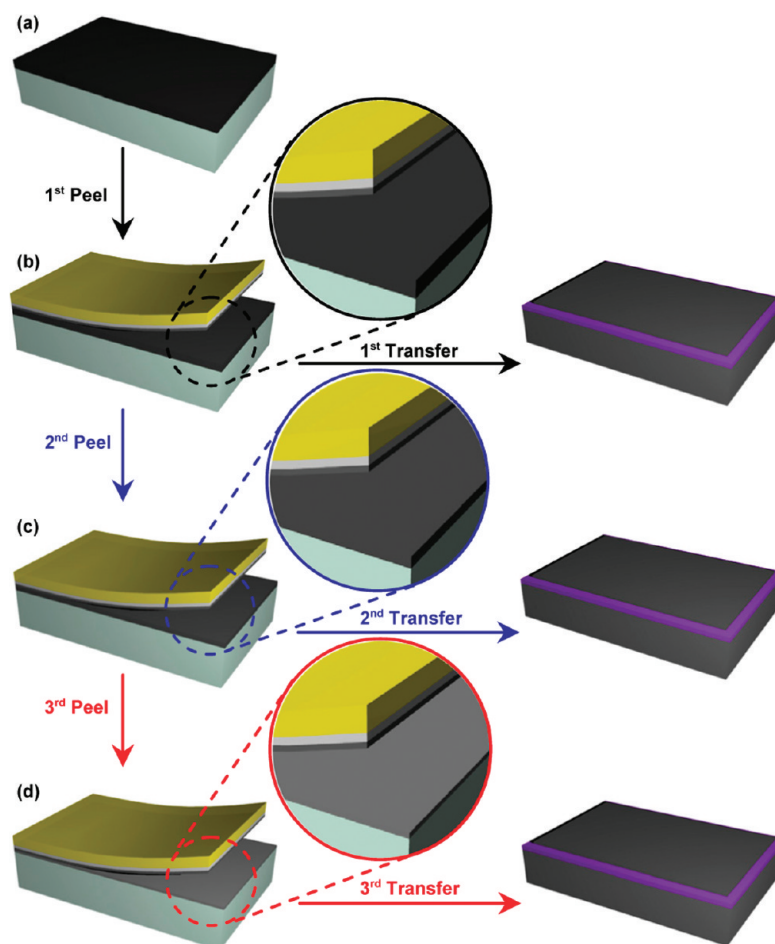


Figure 1. Schematic illustration of procedures for layer-by-layer transfer of graphene grown in a multilayer deposit on a SiC wafer to other substrates. (a) Multilayer graphene grown on the Si face of 6H-SiC. (b) Bilayer of Pd and PI deposited on the SiC as an adhesive layer and mechanical support, respectively, for peeling and gently transferring graphene to a target substrate. Only the top graphene layer is removed and transferred. (c) The same SiC substrate coated again with Pd/PI, followed by transfer to produce another graphene film. (d) Same process repeated a third time.

In the following, we demonstrate a process for sequential transfer of single layers of graphene from multilayer deposits on SiC, over large areas with high yields, enabled by the replacement of Au with Pd. A unique and important feature of the process, as demonstrated explicitly in the following, is that it can be repeated to enable a layer-by-layer transfer of multiple, large area sheets of graphene from a single SiC substrate. Low energy electron diffraction (LEED), X-ray photoelectron spectroscopy (XPS), atomic force microscopy (AFM), scanning tunneling microscopy (STM), scanning tunneling spectroscopy (STS), scanning electron microscopy (SEM), and optical microscopy reveal the nature of the grown and transferred material. Four-point probing of graphene on insulating substrates indicates sheet resistances comparable to those of single-layer graphene derived from CVD on Cu.¹³ In a final example, we demonstrate the ability to manipulate graphene into stacked geometries, as an example of the versatility of these approaches.

RESULTS AND DISCUSSION

Figure 1 illustrates steps for multiple transfers of single-layer graphene from epitaxial material on a

SiC(0001) wafer. The first involves growth on SiC at 1550 °C (Figure 1a), using conditions described in the experimental section. Depositing a thin layer of Pd and then coating with polyimide (PI) prepares the substrate for transfer, where the PI/Pd/graphene film is peeled away manually (Figure 1b) and then gently placed onto a target substrate. Removing the PI film followed by the Pd film leaves only the transferred graphene. Repeating this sequence of steps (except for the graphene growth) with the same SiC substrate allows additional layers of graphene to be removed and transferred (Figure 1c,d). We successfully transferred up to six layers with area yields of almost 100% for the first two or three layers and 30% for the subsequent layers. Details appear in Supporting Information. In the following, we focus on a representative case of two transfers.

The LEED pattern in Figure 2a, corresponding to the SiC(1 × 1) of SiC(0001), and an *ex situ* AFM image (Asylum Research MFP-3D) in Figure 2b show the state of the substrate before growth but after heating overnight at 600 °C. After growth at 1550 °C for 2 h, the substrate formed thick, multilayer graphene deposits, as

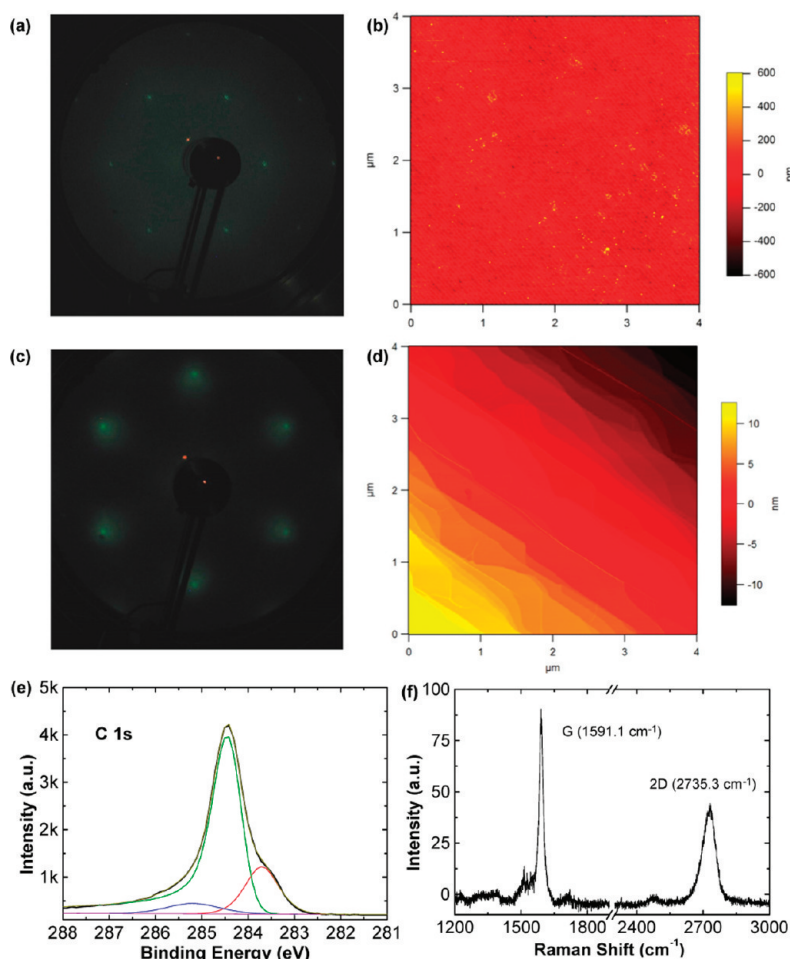


Figure 2. Characterization of a SiC(0001) substrate and epitaxially grown graphene. (a) LEED pattern recorded *in situ* with $E_p = 174.3$ eV on SiC after degassing overnight at 600 °C. The data reveal the expected (1×1) SiC(0001) pattern. (b) A typical $4 \mu\text{m} \times 4 \mu\text{m}$ tapping-mode AFM image of the SiC. (c) LEED pattern with $E_p = 174.7$ eV, collected after growth, showing a (1×1) pattern from graphene. (d) AFM image of graphene on SiC, showing extended terraces and some wrinkles in the graphene. (e) XPS spectrum of the C 1s region of the as-grown sample exhibiting a SiC peak at 283.7 eV, graphene peak at 284.5 eV, and an interface layer peak at 285.2 eV. (f) Background subtracted Raman spectrum showing G and 2D peaks, which suggests multilayer graphene. The D peak was not observed in this sample.

evidenced *in situ* by the expected change in the LEED pattern from that of SiC(1×1), corresponding to the SiC(0001) substrate, to graphite (1×1), corresponding to graphene (Figure 2c).^{21,22} Figure 2d shows an AFM image of a representative $4 \mu\text{m} \times 4 \mu\text{m}$ area. The wrinkles, formed during relaxation of compressive strains induced by cooling, are consistent with previous reports.²³ XPS and Raman spectroscopy data in Figure 2e and 2f, respectively, provide additional data. The three peaks in the C 1s XPS spectrum (Kratos Axis Ultra photoelectron spectrometer) at 283.7 eV (red curve), 284.5 eV (green curve) and 285.2 eV (blue curve) can be assigned to SiC, graphene, and an interface layer, respectively.^{21,24} Thickness calculations that use relative intensities of the SiC and graphene peaks and calculated inelastic mean-free paths of both SiC and graphene at the kinetic energy of the C 1s photoelectron yield a thickness of ~ 2.50 nm. Details on data fitting and calculation are described in Supporting Information. The background-subtracted Raman spectrum

(JY Horiba LabRam HR800) collected with 532 nm excitation through a $100\times$ air objective (laser spot diameter $\sim 1 \mu\text{m}$) shows the expected G and 2D peaks at 1591.1 and 2735.3 cm^{-1} , respectively (Figure 2f).²⁵ Details on spectra correction are also reported in Supporting Information. These positions are blue-shifted compared to those of graphene layers derived from HOPG, consistent with compressive strains mentioned above.²⁵ The width of the 2D peak (FWHM) is 72.6 cm^{-1} , typical for epitaxial graphene whose thickness is larger than bilayer.²⁶ The absence or low intensity of the D peak, which is expected to lie between $1300\text{--}1400 \text{ cm}^{-1}$, suggests that the deposits have a low density of defects.

The transfer processes occurred immediately after such measurements, for each cycle. Figure 3a provides a picture of two large ($\sim 1 \text{ cm}^2$) transferred sheets of graphene derived from a single deposit on SiC, on substrates of SiO_2/Si . The sizes are limited only by those of the SiC pieces and the sample mount in the growth chamber. The low magnification optical micrograph in

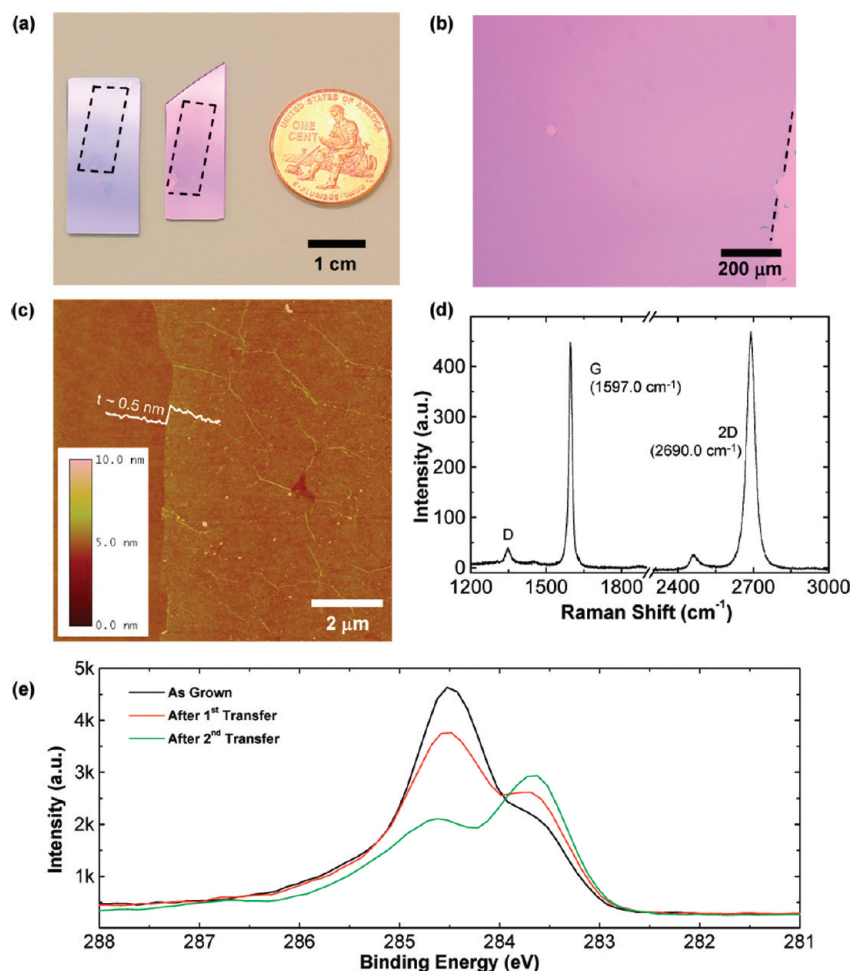


Figure 3. Properties of graphene transferred from SiC to SiO₂(300 nm)/Si. (a) Digital camera image showing two transferred graphene films derived from a single SiC growth substrate. The films are uniform over square centimeter areas. (b) Optical image of a graphene sheet in panel a collected near the edge of the film. (c) AFM image of a representative region indicating a uniform thickness of ~ 0.5 nm. (d) Raman spectrum showing the expected D, G, and 2D peaks. The 2D peak is well-fitted to a single Lorentzian form. (e) C 1s core-level XPS spectra of a SiC substrate collected immediately after growth of graphene (black line), after the 1st transfer step (red line), and after the 2nd transfer step (green line). The peak associated with graphene weakens while one from SiC becomes stronger after each transfer step.

Figure 3b reveals good film uniformity, with a small fold near the edge on the lower right. Imaging by AFM near the edge indicates a thickness of ~ 0.5 nm, as shown in Figure 3c. Raman spectroscopy (Figure 3d) reveals D, G, and 2D peaks at 1347.9, 1597.0 (FWHM = 15 cm⁻¹), and 2690.0 cm⁻¹ (FWHM = 35.3 cm⁻¹), respectively. The appearance of the D peak implies a certain amount of defects, possibly partially introduced by the transfer processing, although still much lower than previous results.¹⁸ The shape of the 2D band matches a single Lorentzian line shape with narrow width (FWHM = 35.3 cm⁻¹); both features are consistent with single layer graphene.^{27–29} Red-shifting of this band relative to that on SiC can be attributed to relaxation of compressive strain upon release. The ratio of the G and 2D bands (I_{2D}/I_G)¹² and the blue-shifting of the G band relative to material on SiC (Figure 3d) are likely influenced by residual doping associated with residues from Pd and/or its etching solution (HCl/FeCl₃-based), consistent with observations in other contexts.^{30,31} Per-

forming XPS on the transferred sheet of graphene revealed the presence of Fe with an atomic percentage of 0.1554; no substantial amount of Pd was observed. C 1s XPS spectra (Figure 3e) collected from the SiC substrate before the first transfer (black), after the first transfer (red), and after the second transfer (green), provide additional evidence for single layer nature of the transferred material. The carbon signals from graphene and SiC decrease and increase, respectively, in a sequential manner. The calculated thicknesses show a decrease in the graphene thickness on SiC from 2.1 to 1.53 nm and 0.68 nm corresponding to the spectra before transfer, after first transfer, and second transfer, respectively. The consistent change in thickness for each transfer suggests a layer-by-layer mode. Although the exact thicknesses are somewhat larger than expectation for single layer graphene, the discrepancies can be attributed to the selection of parameters for the fitting (*i.e.*, the inelastic mean-free path for graphene and SiC). Such outcomes are insensitive to the conditions for

peeling, over the range examined, including various speeds and directions, using tweezers as well as stamps of poly(dimethylsiloxane), both along the length of the substrate and perpendicular to the terrace steps.

To gain unambiguous insights into the nature of the transferred layers, we performed atomic resolution STM, and scanning tunneling spectroscopy (STS). Measurements using a UHV-STM system appear in Figure 4a–d. The results indicate both honeycomb and trigonal lattices, the former of which is expected for single-layer graphene.³² The trigonal symmetry observed in certain regions is likely not due to the presence of multiple layers, since the surrounding area shows hexagonal symmetry and there are no steps in the surface. Rather, this symmetry is likely caused by curvature and local doping of the graphene. Data from STS yields information on the local density of states, through the quantity $(dI/dV)/(I/V)$, as shown in Figure 4e. The blue curve corresponds to an average of ~ 700 spectra recorded on different areas of the surface. The red curve represents similar data collected from a sample of graphene exfoliated from HOPG and deposited on the Si(100) – 2×1 :H surface. Clearly, the graphene synthesized on SiC and transferred to SiO₂ has a higher density of states at low energies. This may result from the expected stronger interaction between graphene and SiO₂, as compared to a fully H-passivated silicon surface. The green curve shows spectra recorded over contamination observed with the STM. The density of states clearly shows that this contamination is metallic and that it might be due to residual Fe from etching solution. The minimum point in the curve for transferred graphene occurs at a slightly positive bias, implying that the film was p doped.

To provide preliminary electrical evaluation and to illustrate an ability to build devices with transferred material, we fabricated arrays of test structures for two- and four-point measurements of sheet resistance. Figure 5 panels a–c show arrays of devices and a magnified view of a representative case. Electrodes 1 and 2 provide a constant current of 0.1 A; electrodes 3 and 4 probe resistive drops in voltage in a region between electrodes 1 and 2. The distance between electrodes 3 and 4 varies from 25 to 100 μm . The results from five different devices on the same film indicate an average sheet resistance of 2.2 k Ω /square, with a variation, from

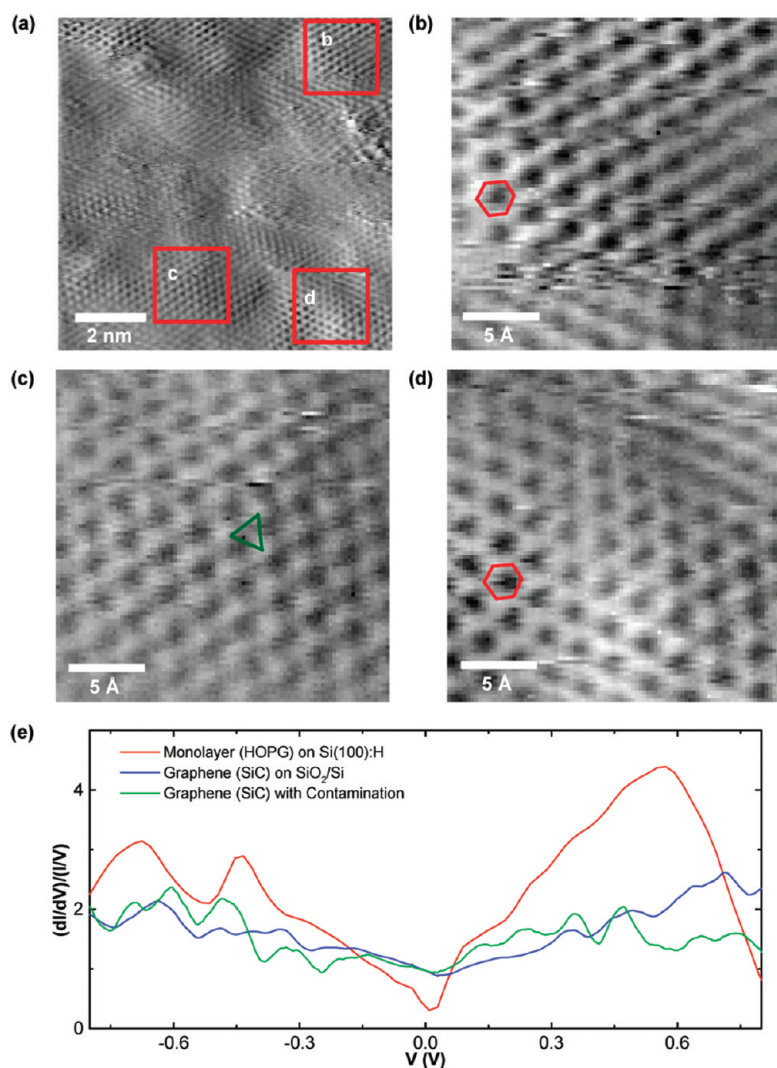


Figure 4. (a) Spatial derivative STM image of the transferred graphene film on SiO₂/Si. $V_{\text{tip-sample}} = -1.5$ V and $I_{\text{tunnel}} = 100$ pA. (b–d) The magnified areas of STM image a. The trigonal structure was observed in image c while honeycomb lattice were observed in images b and d. (e) The plot of density of states derived from $(dI/dV)/(I/V)$ versus voltage (V) from STS of a graphene film derived from HOPG on Si and a transferred graphene film on SiO₂/Si.

maximum to minimum value, of 0.9 k Ω /square. These resistances are comparable to those of single layer graphene grown on Cu¹³ and are much lower than those from chemically derived graphene film from graphene oxide (GO).³³ The sheet resistances determined at these sub-mm scales might be somewhat different than those from large area measurement. More complete studies of the electronic properties represent topics of current work.

To demonstrate additional capabilities of the processes, we built crossbar structures (Figure 6a) by double transfer of pre-patterned graphene films. Here, we first transferred graphene films from one SiC wafer to two different SiO₂/Si substrates. The films were then separately patterned into 100 μm ribbons by photolithography and etching with an O₂ plasma. Finally, the resulting graphene ribbons were transferred from one

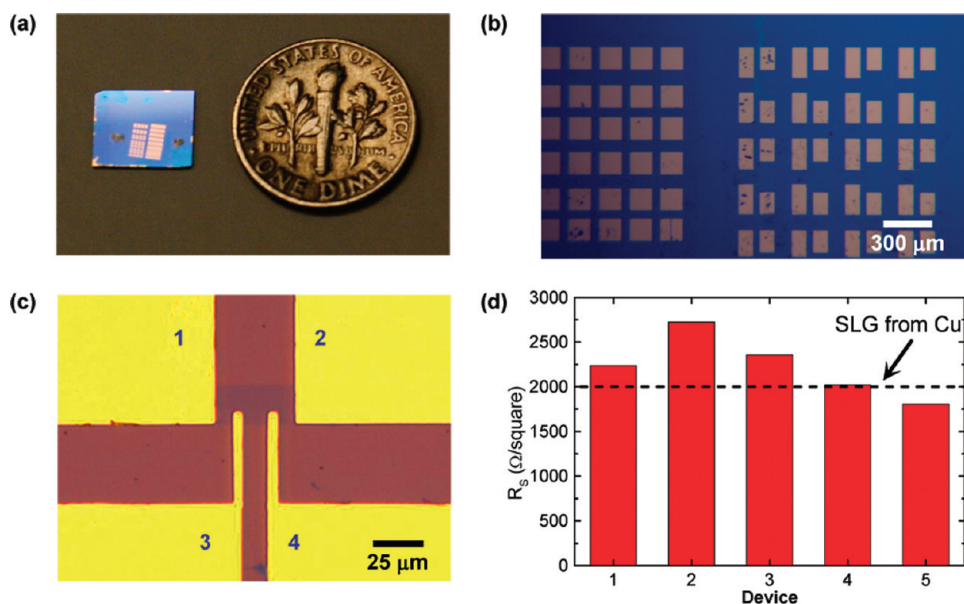


Figure 5. (a) Digital camera image showing arrays of devices fabricated on a film of graphene transferred to a SiO_2/Si substrate. (b) Low magnification optical image of some devices. (c) Representative optical image of a device configured for four-point probing, with notation identifying each Cr/Au contact. (d) Sheet resistances determined from several different devices.

of the SiO_2/Si substrates to the other in a manner that aligned the ribbons in an orthogonal fashion. The SEM image (Hitachi S-4800 FE-SEM) in Figure 6b reveals only a few tears associated with this double transfer proce-

dure. Figure 6 panels c and d present height and phase mode AFM images from the same $20\ \mu\text{m} \times 20\ \mu\text{m}$ AFM scan. The thickness of the vertical ribbon was *ca.* 0.5–0.6 nm.

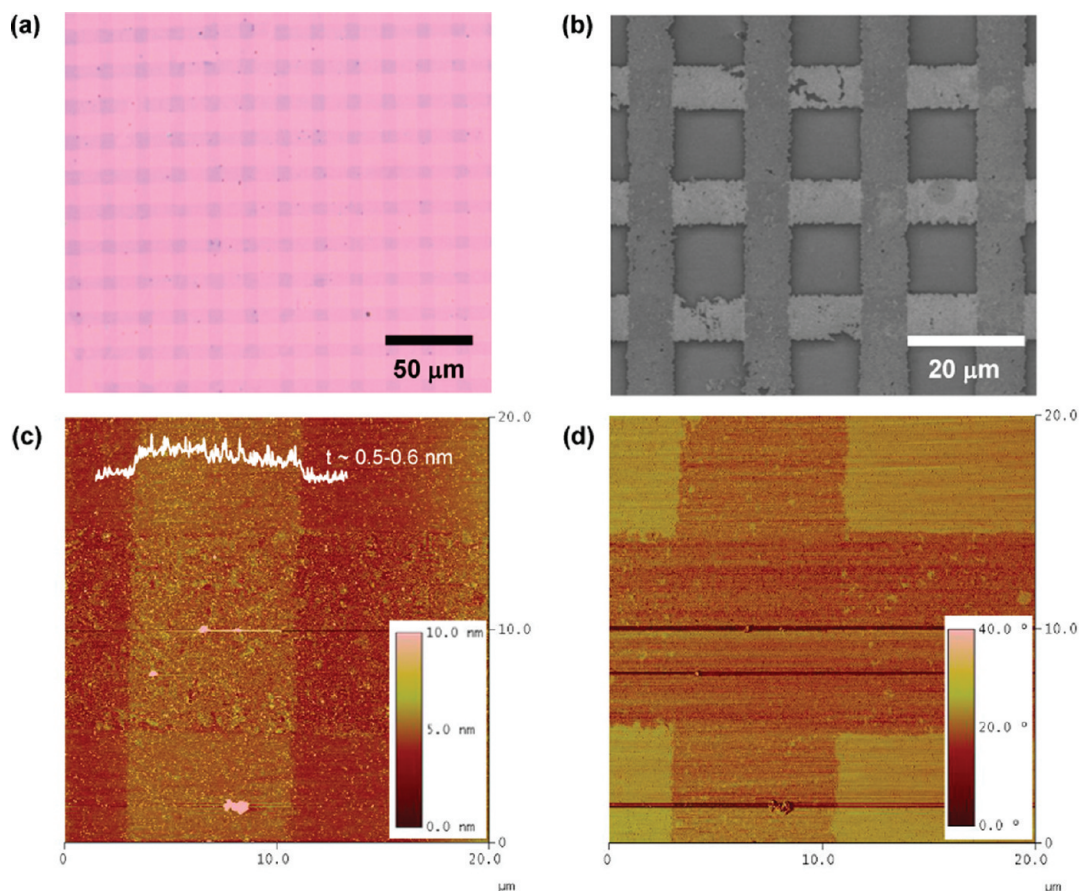


Figure 6. (a) A graphene crossbar structure fabricated by transferring patterned graphene twice with perpendicular alignment. (b) Low magnification SEM image of graphene crossbar structure. (c) Height mode and (d) phase mode AFM images of the same structure.

CONCLUSIONS

The transfer techniques reported here offer an ability to produce multiple, large area, single-layer graphene films from multilayer deposits on a SiC substrate. These outcomes might be useful for the creation of single-layer graphene from SiC and for its heterogeneous integration, for example, into a

silicon-based electronics platform. Multilayer configurations as well as use on plastic substrates for flexible electronics and other unconventional applications could also be valuable. Exploring these possibilities and characterizing further the electrical and mechanical properties of the materials are topics of current work.

EXPERIMENTAL METHODS

Epitaxial Growth of Graphene Layers on SiC Substrates. The growth used rectangular (5 mm × 25 mm) pieces of SiC(0001) wafers (II–VI, Inc.) coated with layers of Ta (200 nm; electron beam evaporation; Temescal BJD1800) on their back sides (C-face) to serve as heating elements. Each substrate was loaded into a UHV chamber (2×10^{-9} Torr) and heated, *via* current passed through the Ta, overnight at 600 °C, monitored by an infrared thermometer (CHINO IR-CAQ; $\epsilon = 0.90$). Increasing the temperature to 1400 °C under a flux of Si (Si_2H_6 ; 2×10^{-6} Torr) improved the surface morphology for the growth step.³⁴ Annealing under atomic hydrogen (4.2×10^{-6} Torr) at 1550 °C for 2 h finished the growth.

Transfer Process of Graphene Layers from SiC Substrates. After growth, a SiC substrate was deposited with a thin layer of Pd (100 nm; electron beam evaporation; Temescal BJD1800) followed by coating with polyimide (PI; *ca.* 1.4 μm , from poly(pyromellitic dianhydride-co-4,4'-oxidianiline) amic acid solution spun cast at 3000 rpm for 30 s, partially cured at 110 °C for 2 min). Next, the PI/Pd/graphene film was peeled away manually and then smoothly placed onto a substrate, such as SiO₂/Si substrate (300 nm SiO₂, Process Specialties, Inc.). Removing the PI film by reactive ion etching (March RIE; 20 sccm O₂, 150 mTorr, 150 W, 30 min) followed by the Pd film by wet etching using a commercially available HCl/FeCl₃-based chemistry (Pd Etchant TFP, Transene, Inc.) left only the transferred graphene on the substrate.

Sample Preparation for STM measurement. A layer of graphene was transferred onto a Si substrate with 300 nm thermal oxide, and then cut to a size of 2 mm × 8 mm. Electrodes of Au (60 nm; electron beam evaporation; Temescal BJD1800) evaporated onto both ends provided electrical connections.

Device Fabrication for Sheet Resistance Measurement. The electrodes were defined by photolithography followed by Cr/Au deposition (5 nm/50 nm) using an electron beam evaporator and lift-off in acetone. Oxygen plasma etching (Plasma Cleaner PDC-32G, Harrick Plasma, Inc.; 200 mTorr, medium RF level, 3 min) removed the graphene outside of the device channel, using a patterned layer of photoresist as a mask, to electrically isolate each device. Finally, the photoresist film was removed by using *n*-methyl-2-pyrrolidone based solvent stripper (Remover PG, MicroChem Corp.) The sample was rinsed with isopropyl alcohol and dried with N₂ gas flow.

Acknowledgment. This work is supported by the U.S. Department of Energy, Division of Materials Sciences under Award No. DE-FG02-07ER46471, through the Materials Research Laboratory and Center for Microanalysis of Materials (DE-FG02-07ER46453) at the University of Illinois at Urbana–Champaign. S.U. was supported, partly, by the Anandamahidol Foundation. S.U. and F.D. also thank Vania Petrova for the use of an infrared thermometer.

Supporting Information Available: Graphene overlayer thickness calculation; Raman spectra. This material is available free of charge *via* the Internet at <http://pubs.acs.org>.

REFERENCES AND NOTES

- Novoselov, K. S.; Geim, A. K.; Morozov, S. V.; Jiang, D.; Zhang, Y.; Dubonos, S. V.; Grigorieva, I. V.; Firsov, A. A. Electric Field Effect in Atomically Thin Carbon Films. *Science* **2004**, *306*, 666–669.
- Novoselov, K. S.; Geim, A. K.; Morozov, S. V.; Jiang, D.; Katsnelson, M. I.; Grigorieva, I. V.; Dubonos, S. V.; Firsov, A. A. Two-Dimensional Gas of Massless Dirac Fermions in Graphene. *Nature* **2005**, *438*, 197–200.
- Zhang, Y.; Tan, J. W.; Stormer, H. L.; Kim, P. Experimental Observation of the Quantum Hall Effect and Berry's Phase in Graphene. *Nature* **2005**, *438*, 201–204.
- Young, A. F.; Kim, P. Quantum Interference and Klein Tunnelling in Graphene Heterojunctions. *Nat. Phys.* **2009**, *5*, 222–226.
- Geim, A. K.; Novoselov, K. S. The Rise of Graphene. *Nat. Mater.* **2007**, *6*, 183–191.
- Geim, A. K. Graphene: Status and Prospects. *Science* **2009**, *324*, 1530–1534.
- Berger, C.; Song, Z.; Li, T.; Li, X.; Ogbazghi, A. Y.; Feng, R.; Dai, Z.; Marchenkov, A. N.; Conrad, E. H.; First, P. N.; de Heer, W. A. Ultrathin Epitaxial Graphite: 2D Electron Gas Properties and a Route toward Graphene-Based Nanoelectronics. *J. Phys. Chem. B* **2004**, *108*, 19912–19916.
- Berger, C.; Song, Z.; Li, X.; Wu, X.; Brown, N.; Naud, C.; Mayou, D.; Li, T.; Hass, J.; Marchenkov, A. N.; *et al.* Electronic Confinement and Coherence in Patterned Epitaxial Graphene. *Science* **2006**, *312*, 1191–1196.
- First, P. N.; de Heer, W. A.; Seyller, T.; Berger, C.; Strosio, J. A.; Moon, J.-S. Epitaxial Graphenes on Silicon Carbide. *MRS Bull.* **2010**, *35*, 296–305.
- Reina, A.; Jia, X.; Ho, J.; Nezich, D.; Son, H.; Bulovic, V.; Dresselhaus, M. S.; Kong, J. Large Area, Few-Layer Graphene Films on Arbitrary Substrates by Chemical Vapor Deposition. *Nano Lett.* **2009**, *9*, 30–35.
- Kim, K. S.; Zhao, Y.; Jang, H.; Lee, S. Y.; Kim, J. M.; Kim, K. S.; Ahn, J.-H.; Kim, P.; Choi, J.-Y.; Hong, B. H. Large-Scale Pattern Growth of Graphene Films for Stretchable Transparent Electrodes. *Nature* **2009**, *457*, 706–710.
- Li, X.; Cai, W.; An, J.; Kim, S.; Nah, J.; Yang, D.; Piner, R.; Velamakanni, A.; Jung, I.; Tutuc, E.; *et al.* Large-Area Synthesis of High-Quality and Uniform Graphene Films on Copper Foils. *Science* **2009**, *324*, 1312–1314.
- Li, X.; Zhu, Y.; Cai, W.; Borysiak, M.; Han, B.; Chen, D.; Piner, R. D.; Colombo, L.; Ruoff, R. S. Transfer of Large-Area Graphene Films for High-Performance Transparent Conductive Electrodes. *Nano Lett.* **2009**, *9*, 4359–4363.
- Bae, S.; Kim, H.; Lee, Y.; Xu, X.; Park, J.-S.; Zheng, Y.; Balakrishnan, J.; Lei, T.; Kim, H. R.; Song, Y. I.; *et al.* Roll-to-Roll Production of 30-Inch Graphene Films for Transparent Electrodes. *Nat. Nanotechnol.* **2010**, *5*, 574–578.
- Kedzierski, J.; Hsu, P.-L.; Healey, P.; Wyatt, P. W.; Keast, C. L.; Sprinkle, M.; Berger, C.; de Heer, W. A. Epitaxial Graphene Transistors on SiC Substrates. *IEEE Trans. Electron Devices* **2008**, *55*, 2078–2085.
- Lin, Y.-M.; Dimitrakopoulos, C.; Jenkins, K. A.; Farmer, D. B.; Chiu, H.-Y.; Grill, A.; Avouris, P. 100-GHz Transistors from Wafer-Scale Epitaxial Graphene. *Science* **2010**, *327*, 662.
- Sprinkle, M.; Ruan, M.; Wu, X.; Hu, Y.; Rubio-Roy, M.; Hankinson, J.; Madiomanana, N. K.; Berger, C.; de Heer, W. A. Directed Self-Organization of Graphene Nanoribbons on SiC. arXiv:1002.0775v1. [cond-mat.mtrl-sci].
- Unarunotai, S.; Murata, Y.; Chialvo, C. E.; Kim, H.-S.; MacLaren, S.; Mason, N.; Petrov, I.; Rogers, J. A. Transfer of Graphene Layers Grown on SiC Wafers to Other Substrates

- and Their Integration into Field Effect Transistors. *Appl. Phys. Lett.* **2009**, *95*, 202101.
19. Caldwell, J. D.; Anderson, T. J.; Culbertson, J. C.; Jernigan, G. G.; Hobart, K. D.; Kub, F. J.; Tadjer, M. J.; Tedesco, J. L.; Hite, J. K.; Mastro, M. A.; *et al.* Technique for the Dry Transfer of Epitaxial Graphene onto Arbitrary Substrates. *ACS Nano* **2010**, *4*, 1108–1112.
 20. Kang, S. J.; Kocabas, C.; Kim, H.-S.; Cao, Q.; Meitl, M. A.; Khang, D.-Y.; Rogers, J. A. Printed Multilayer Superstructures of Aligned Single-Walled Carbon Nanotubes for Electronic Applications. *Nano Lett.* **2007**, *7*, 3343–3348.
 21. Rollings, E.; Gweon, G.-H.; Zhou, S. Y.; Mun, B. S.; McChesney, J. L.; Hussain, B. S.; Fedorov, A. V.; First, P. N.; de Heer, W. A.; Lanzara, A. Synthesis and Characterization of Atomically Thin Graphite Films on a Silicon Carbide Substrate. *J. Phys. Chem. Solids* **2006**, *67*, 2172–2177.
 22. Hass, J.; de Heer, W. A.; Conrad, E. H. The Growth and Morphology of Epitaxial Multilayer Graphene. *J. Phys.: Condens. Matter* **2008**, *20*, 323202.
 23. Sun, G. F.; Jia, J. F.; Xue, Q. K.; Li, L. Atomic-Scale Imaging and Manipulation of Ridges on Epitaxial Graphene on 6H-SiC(0001). *Nanotechnology* **2009**, *20*, 355701.
 24. Biedermann, L. B.; Bolen, M. L.; Capano, M. A.; Zemlynov, D.; Reifengerger, R. G. Insights into Few-Layer Epitaxial Graphene Growth on 4H-SiC(0001) Substrates from STM Studies. *Phys. Rev. B* **2009**, *79*, 125411.
 25. Röhl, J.; Hundhausen, M.; Emtsev, K. V.; Seyller, T.; Graupner, R.; Ley, L. Raman Spectra of Epitaxial Graphene on SiC(0001). *Appl. Phys. Lett.* **2008**, *92*, 201918.
 26. Lee, D. S.; Riedl, C.; Krauss, B.; von Klitzing, K.; Starke, U.; Smet, J. H. Raman Spectra of Epitaxial Graphene on SiC and of Epitaxial Graphene Transferred to SiO₂. *Nano Lett.* **2008**, *8*, 4320–4325.
 27. Ferrari, A. C.; Meyer, J. C.; Scardaci, V.; Casiraghi, C.; Lazzeri, M.; Mauri, F.; Piscanec, S.; Jiang, D.; Novoselov, K. S.; Roth, S.; Geim, A. K. Raman Spectrum of Graphene and Graphene Layers. *Phys. Rev. Lett.* **2006**, *97*, 187401.
 28. Emtsev, K. V.; Bostwick, A.; Horn, K.; Jobst, J.; Kellogg, G. L.; Ley, L.; McChesney, J. L.; Ohta, T.; Reshanov, S. A.; Röhl, J.; *et al.* Towards Wafer-Size Graphene Layers by Atmospheric Pressure Graphitization of Silicon Carbide. *Nat. Mater.* **2009**, *8*, 203–207.
 29. Malard, L. M.; Pimenta, M. A.; Dresselhaus, G.; Dresselhaus, M. S. Raman Spectroscopy in Graphene. *Phys. Rep.* **2009**, *473*, 51–87.
 30. Das, A.; Pisana, S.; Chakraborty, B.; Piscanec, S.; Saha, S. K.; Waghmare, U. V.; Novoselov, K. S.; Krishnamurthy, H. R.; Geim, A. K.; Ferrari, A. C.; Sood, A. K. Monitoring Dopants by Raman Scattering in an Electrochemically Top-Gated Graphene Transistor. *Nat. Nanotechnol.* **2008**, *3*, 210–215.
 31. Jung, N.; Kim, N.; Jockusch, S.; Turro, N. J.; Kim, P.; Brus, L. Charge Transfer Chemical Doping of Few Layer Graphenes: Charge Distribution and Band Gap Formation. *Nano Lett.* **2009**, *9*, 4133–4137.
 32. Ishigami, M.; Chen, J. H.; Cullen, W. G.; Fuhrer, M. S.; Williams, E. D. Atomic Structure of Graphene on SiO₂. *Nano Lett.* **2007**, *7*, 1643–1648.
 33. Wu, J.; Agrawal, M.; Becerril, H. A.; Bao, Z.; Liu, Z.; Chen, Y.; Peumans, P. Organic Light-Emitting Diodes on Solution-Processed Graphene Transparent Electrodes. *ACS Nano* **2010**, *4*, 43–48.
 34. Tromp, R. M.; Hannon, J. B. Thermodynamics and Kinetics of Graphene Growth on SiC(0001). *Phys. Rev. Lett.* **2009**, *102*, 106104.